THE EFFECT OF PLASMA LOADING ON IMPEDANCE AS OBSERVED IN AN INDUCTIVELY COUPLED PLASMA SOURCE

by

Melissa Wessels

Memorandum No. UCB/ERL M96/49

11 September 1996

THE EFFECT OF PLASMA LOADING ON IMPEDANCE AS OBSERVED IN AN INDUCTIVELY COUPLED PLASMA SOURCE

by

Melissa Wessels

Memorandum No. UCB/ERL M96/49

11 September 1996

ELECTRONICS RESEARCH LABORATORY

College of Engineering
University of California, Berkeley
94720

The Effect of Plasma Loading on Impedance as Observed in an Inductively Coupled Plasma Source

Melissa Wessels
Department of Physics, Smith College, Northampton, MA

Inductive discharges have been studied using a Transformer Coupled Plasma source driven at 13.56 MHz, where the inductive coupling process between the driving coil and the plasma is modeled as an air-core transformer. The effect of the plasma loading is seen in the primary circuit as a change in the impedance by an amount of $\rho + j\chi$. The purpose of the investigation is to observe this effect, and the correlations between ρ and χ, and the absorbed power. This is achieved by relating the external electrical quantities of voltage, current, and transmitted power, and the calculated characteristics of the driving coil. In order to accomplish this task, a shielded voltage divider was designed and constructed to produce reliable voltage measurements despite the large amount of rf interference produced by the high-power rf inductive coupling. A correlation between ρ and the absorbed power was observed, with increasing change in primary resistance for increased absorbed power. A correlation between the change in the primary reactance and the absorbed power was not observed. This may be due to the large error present in the transmitted power measurements.

I. Introduction

This study is part of a larger investigation that seeks to better understand the physics of high-density, inductive discharges now being used for materials processing.[1] In an inductively coupled plasma source, the plasma is produced by applying a radio-frequency voltage across a non-resonant driving coil. The process gas near the coil experiences breakdown as electrons within the gas gain energy in the induced electric field, and are able to ionize neutral atoms through collision. This process is modeled as an air-core transformer, where the driving coil is the primary circuit, and the plasma acts as the secondary circuit. Figure 1 illustrates this coupling.

---

[1]J.T. Gudmundsson and M.A. Lieberman (1996) *A Simple Transformer Model Applied to a Planar Inductive Plasma Discharge*, Memorandum No. UCB/ERL M96/3, University of California, Berkeley

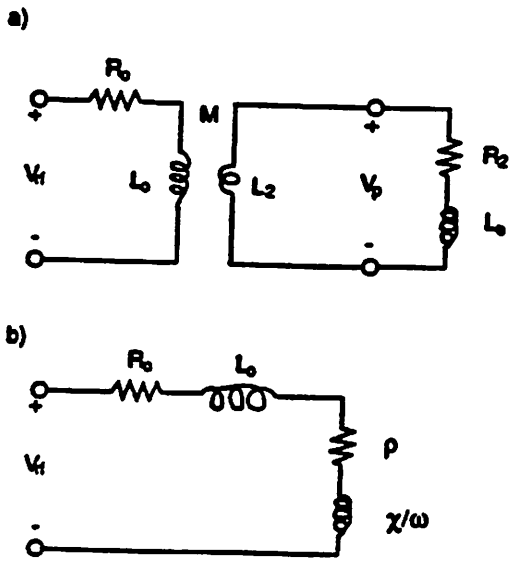

Fig.1[2]: The transformer circuit. (a) The primary circuit has inductance L_0 and resistance R_0 and the secondary circuit consists of geometric inductance L_2, electron inertia inductance L_e and the plasma resistance R_2. (b) The secondary circuit transformed into the primary circuit. The change in primary circuit impedance due to plasma loading is $\rho + j\chi$.

R_0 and L_0 are the resistance and the inductance of the driving coil, respectively. R_2 is the plasma resistance. L_2 is the geometric inductance of the plasma, and is due to the plasma current path. L_e is the electron inertia inductance. As seen when the secondary circuit is transformed into the primary circuit, the effect of plasma loading is a change in the impedance of the primary circuit by an amount $\rho + j\chi$.

This investigation seeks to observe this effect, and to determine the values of ρ and χ, as they relate to the coil characteristics as seen with and without plasma coupling, and the applied external electrical quantities of power, voltage, and current. To accomplish this objective, a shielded voltage divider has been designed and constructed to yield reliable voltage measurements despite the large amount of rf interference due to the high-power rf inductive coupling.

II. Apparatus and Procedure

The Transformer Coupled Plasma Source

Figure 2 is a schematic of the Transformer Coupled Plasma (TCP) source used to conduct the experiment.

---

[2]Ibid., p. 3

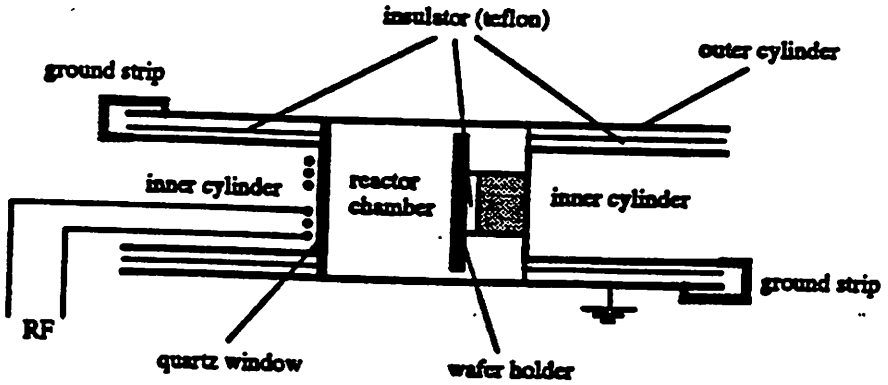

Fig.2[3]: Schematic of the TCP source.

The source is powered by a 1 kW Henry 1000D Radio Frequency Power Generator connected to an L-type capacitive matching network at a driving frequency of 13.56 MHZ[4]. The primary coil that is coupled to the plasma is a three-turn, copper coil, 0.06 cm thick, and 1.9 cm wide, with an outer radius of 9.09 cm, and even spacing between turns. It is placed 0.3 cm away from a quartz dielectric window, 2.5 cm in thickness, which separates the coil from the vacuum chamber where argon gas is fed. The rf current in the coil induces an electric field within the gas- filled vacuum chamber, thereby initiating the breakdown process, and producing an argon plasma. The plasma then streams toward the wafer where the materials processing is done.

Voltage Divider Circuit Design

The voltage divider monitors the voltage across the primary coil from its high voltage point at its center to the outer edge of the coil which is attached to ground. It is designed to produce output voltages that can be viewed and measured on a HP 54600A oscilloscope. The voltages across the coil vary up to 1400 V, while the oscilloscope has a maximum voltage input of 400 V. Furthermore, shielding was required in order to avoid the large amount of rf interference, whereby stray voltages produced by capacitive or inductive coupling between the voltage divider circuit and the matching network elements can produce inaccurate voltage readings. Figure 3 is a diagram of the voltage divider circuit.

---

[3]Gianluca Gregori and M.A. Lieberman (1996) *RF Plasma Potential and Surface Temperature Measurements in an Inductively Coupled Plasma Source*, Memorandum No. UCB/ERL M96/14, University of California, Berkeley, p.2

[4]See Gudmundsson and Lieberman, p. 3

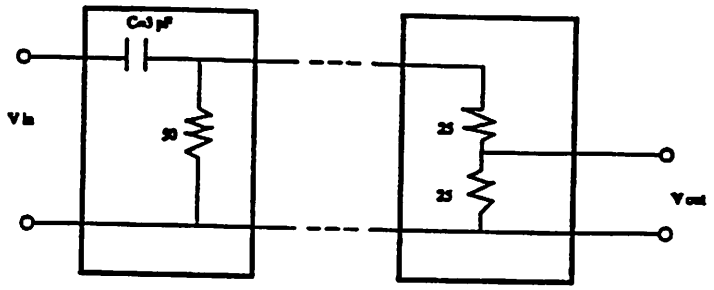

Fig. 3: The voltage divider circuit diagram. The boxes indicate shielding, while the dotted lines indicate where coaxial cable connections were made.

The shielding was accomplished by encasing the circuit components within two small grounded aluminum boxes, as indicated in figure 3. The boxes were connected by coaxial cable with a characteristic impedance of 50 ohms. Inside the matching network, a coaxial cable with a solid copper outer conductor was used to connect the right edge of the first box to the outside of the network, to ensure proper shielding. From the matching network to the second box, outside the TCP source, approximately six feet of braided coax was used with an outer braid around, forming a triax system. The braided coax connects to the second box which is attached to an oscilloscope by a BNC-type connector. The nominal 3 pF capacitor was kept just outside the first box because it carries high voltage on its anode. A wire lead from the capacitor, 6 cm in length, was required to connect the voltage divider to the center of the coil. Associated with the wire lead is some additional capacitance. The capacitance across the capacitor and this lead was measured using a HP 8753A Network Analyzer. The measured value was 3.9 pF ± 0.2 pF. Therefore, the lead adds approximately 0.9 pF to the nominal capacitance of the circuit.

Calibration of the Voltage Divider

Analyzing the voltage divider circuit, the output voltage, Vout, can be written as

$$V_{OUT} = 25\, I \tag{1}$$

where

$$I = \frac{1}{2} I_{IN} = \frac{V_{IN}}{(50 + \frac{2}{j\omega C})} \tag{2}$$

Substituting (2) into equation (1),

$$V_{OUT} = (\frac{25\, j\omega C}{50\, j\omega C + 2})\, V_{IN} = (\frac{50\, j\omega C + 1250\, \omega^2 C^2}{4 + 2500\, \omega^2 C^2})\, V_{IN} \tag{3}$$

Therefore, the ratio of the amplitudes of V_{OUT} and V_{IN} can be written as

$$\frac{|V_{OUT}|^2}{|V_{IN}|^2} = \left(\frac{50\ \omega C}{4 + 2500\ \omega^2 C^2}\right)^2 + \left(\frac{1250\ \omega^2 C^2}{4 + 2500\ \omega^2 C^2}\right)^2 \quad (4)$$

The voltage division, $D=V_{OUT}/V_{IN}$, was calculated as a function of frequency, f, where f is equal to the angular frequency, ω, divided by 2π. These calculations used 3.9 pF for the value of C, taking into account the capacitance of the unshielded lead. The calculated theoretical values were then compared to experimental values measured with the network analyzer. The network analyzer applies an input voltage and measures the voltage division factor, D, in dB. Ten measurements were taken at each of 16 different frequencies, and the average and standard error were calculated. The theoretical and experimental values are summarized in Table 1, where the voltage division is recorded in dB. Note that $D_{dB} = 20 \log D$.

Frequency [MHZ]	Voltage Division (Theoretical) [dB]	Voltage Division (Experimental) [dB]
3	-60.7	-59.7
5	-56.3	-55.5
7	-53.4	-52.6
9	-51.2	-50.4
11	-49.4	-48.7
13	-48.0	-47.3
13.56	-47.6	-47.0
15	-46.8	-46.2
17	-45.7	-45.3
19	-44.7	-44.3
21	-43.8	-43.3
23	-43.0	-42.5
25	-42.3	-41.7
27	-41.7	-41.1
29	-41.0	-40.3
31	-40.5	-39.7

Table 1: A comparison of the theoretical and experimental values for the voltage division vs. frequency. The reported experimental values are the calculated averages of ten measurements taken at each frequency. The standard error in the experimental values varies from 0.04% to 0.2%.

Figure 4 is a plot of voltage division vs. frequency. The small discrepancy between the theoretical and experimental values is due to the added capacitance of the unshielded lead. Using the measured experimental values, C was calculated at each frequency. The average value of C was found to be 4.2 pF ± 0.1 pF. This value is within the uncertainty of the measured value of C, 3.9 pF ± 0.2 pF.

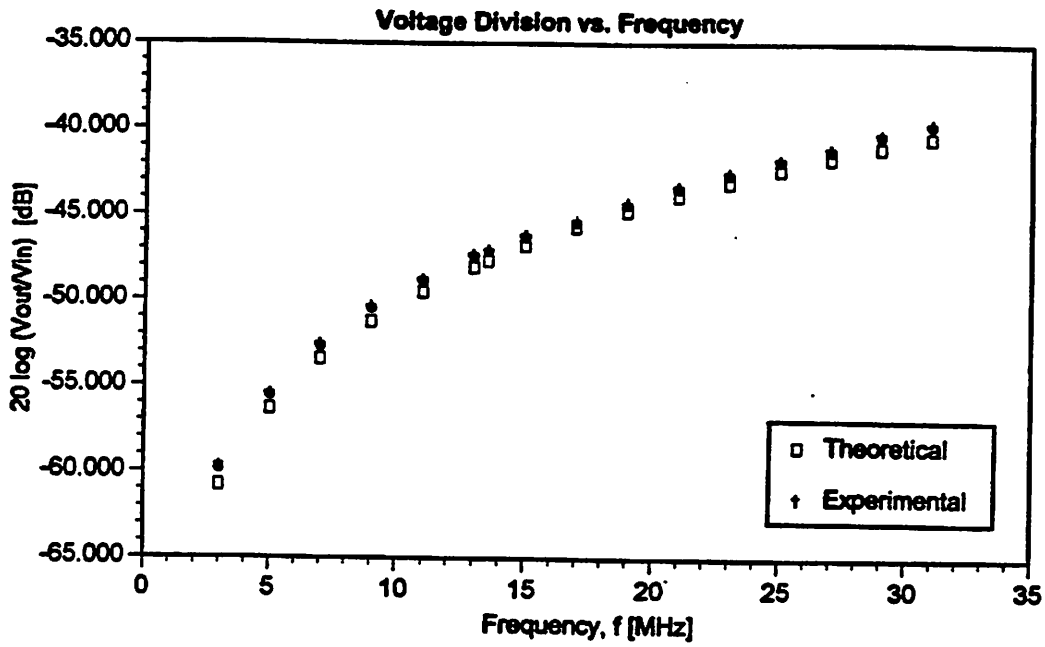

Fig. 4: A plot of voltage division as a function of frequency. The uncertainty in the frequency is estimated to be ±0.01 MHz.

Of particular interest is the voltage division factor at the frequency of 13.56 MHZ, the driving frequency of the plasma source. The measured value of D_{dB} at 13.56 MHZ is -47.01 dB ± 0.02 dB. This corresponds to a value of D at 13.56 MHZ equal to 0.00446 ± 1E-5.

The Experiment

The voltage divider was soldered into the matching network as shown in figure 5.

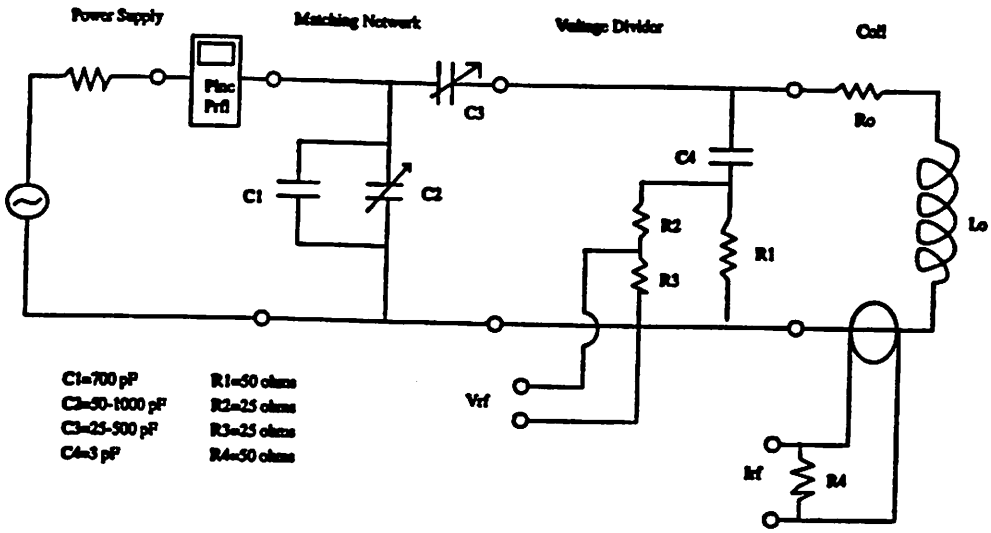

Fig. 5: The circuit diagram showing the power supply, the matching network, the voltage divider, and the inductive coil.

The current is monitored with a Pearson coil, model 411. Both the current and the voltage signals are displayed on an oscilloscope. A Bird Electronics Model 43 watt meter measures the incident power flow to the coil, P_{inc}, and the reflected power, P_{rfl}. The power dissipated in the coil then, P, is the difference between these two readings, $P = P_{inc} - P_{rfl}$. The first set of data was recorded when no plasma was present in the reaction chamber. The power was varied between 30 W and 250 W, and the matching network was tuned at each increment to ensure maximum power transfer ($P_{rfl} << P_{inc}$) from the supply to the inductive coil. At each power increment, the peak to peak voltage, V_{p-p}, and current, I_{p-p}, were measured on the oscilloscope. Next, an argon plasma was initiated in the reaction chamber. The experiment was repeated for gas pressures of 10, 30, and 50 mTorr, and for power increments between 20W and 700W. For each power increment, at each pressure, V_{p-p} and I_{p-p} were recorded. The error in the power measurements is estimated to be ±5% of the measurement due to reading error, plus an instrument error of ±5% of the power meter scale's full range. The incident power scale measured a maximum of 1000 W, while the reflected power scale measured a maximum of 50 W. The uncertainties in V_{p-p} and I_{p-p} are estimated to be ±0.1V.

III. Observations and Analysis

Table 2 contains the raw data collected for the experiment conducted when no plasma was present, along with the calculated root-mean-square values of V_{rf} and I_{rf}. V_{rf} and I_{rf} are given by the following equations.

$$V_{rf} = \frac{V_{p-p}}{2\sqrt{2} * D} \tag{5}$$

$$I_{rf} = \frac{I_{p\text{-}p} * C}{2\sqrt{2} * K} \tag{6}$$

D is the voltage division factor 0.00446 ± 1E-5. C is the calibration coefficient, equal to 20 A/V. It is the product of the current monitor specification and a factor of two due to a 50 ohm terminator that was used during measurements. K is the high frequency response and is designed to compensate for a shift in calibration at high frequencies. The value of K is 1.616 and was obtained from a calibration chart produced by Pearson. The uncertainties in V_{rf} and I_{rf} are given by equations (7) and (8). The uncertainty in V_{rf} varies from 0.5% to 1%, while the uncertainty in I_{rf} ranges from 1% to 3%.

$$(\sigma_{V_{rf}})^2 = (\sigma_{V_{p\text{-}p}})^2 \left(\frac{\partial V_{rf}}{\partial V_{p\text{-}p}}\right)^2 + (\sigma_D)^2 \left(\frac{\partial V_{rf}}{\partial D}\right)^2 \tag{7}$$

$$(\sigma_{I_{rf}})^2 = (\sigma_{I_{p\text{-}p}})^2 \left(\frac{\partial I_{rf}}{\partial I_{p\text{-}p}}\right)^2 \tag{8}$$

P [W]	$V_{p\text{-}p}$ [V]	V_{rf} [V]	$I_{p\text{-}p}$ [V]	I_{rf} [A]
30	7.8	618.3	2.6	11.4
50	8.4	665.9	2.8	12.3
65	10.8	856.1	3.5	15.3
80	12.0	951.3	3.9	17.1
100	13.0	1030.5	4.1	17.9
135	14.3	1133.6	4.6	20.1
185	16.4	1300.1	5.3	23.2
200	17.0	1347.6	5.5	24.1
230	18.1	1434.8	5.8	25.4
250	18.9	1498.2	6.0	26.3

Table 2: Measured and calculated values of voltage and current as a function of power, when no plasma is present within the reaction chamber.

This data yields the values of R_0 and L_0, and allows for a comparison to the data collected when a plasma is present in the chamber, and subsequently for the calculation of the change in primary resistance, ρ, and reactance, χ, due to plasma loading. When no plasma is present, the ratio of the voltage to the current in the primary of the transformer circuit of figure 1 can be written as

$$\frac{V_{rf}}{I_{rf}} = R_0 + j\omega L_0 \tag{9}$$

Therefore,

$$\frac{|V_{rf}|^2}{|I_{rf}|^2} = R_0^2 + \omega^2 L_0^2 = (\frac{P}{|I_{rf}|^2})^2 + \omega^2 L_0^2 \tag{10}$$

And solving for L_0,

$$L_0^2 = (\frac{|V_{rf}|^2}{|I_{rf}|^2} - (\frac{P}{|I_{rf}|^2})^2) / \omega^2 \tag{11}$$

Then, R_0 can be found, where

$$R_0 = \frac{P}{|I_{rf}|^2} \tag{12}$$

Table 3 shows the calculated values of L_0 and R_0 as a function of power along with their averages. The average value of L_0 is 657.0 nH ± 3.7 nH, while the average value of R_0 is 0.10 Ω ± 0.01Ω. The uncertainty in each of these values was found as the standard error.

P[W]	Lo[nH]	Ro[Ω]
30	637.9	0.05
50	637.9	0.11
65	656.1	0.08
80	654.3	0.07
100	674.2	0.09
135	661.0	0.11
185	658.0	0.12
200	657.2	0.12
230	663.6	0.13
250	669.8	0.13
AVG	657.0	0.10

Table 3: L_0 and R_0 as a function of power, and their calculated averages.

The raw data collected for the experiment performed with plasma present within the reactor chamber is summarized in Table 4, along with the calculated rms values of voltage and current.

	10 mTorr				30 mTorr				50 mTorr			
P [W]	V_{p-p} [V]	V_{rf} [V]	I_{p-p} [V]	I_{rf} [A]	V_{p-p} [V]	V_{rf} [V]	I_{p-p} [V]	I_{rf} [A]	V_{p-p} [V]	V_{rf} [V]	I_{p-p} [V]	I_{rf} [A]
20	6.0	475.6	1.9	8.3	6.1	483.6	2.0	8.8	5.8	459.8	1.9	8.3
50	8.6	681.7	2.9	12.7	7.2	570.8	2.4	10.5	6.7	531.1	2.2	9.6
80	8.6	681.7	2.9	12.7	7.5	594.5	2.4	10.5	6.8	539.1	2.3	10.1
100	9.1	721.4	3.0	13.1	7.7	610.4	2.6	11.4	7.5	594.5	2.5	10.9
200	10.9	864.1	3.6	15.8	9.4	745.2	3.2	14.0	9.2	729.3	3.1	13.6
300	12.5	990.9	4.1	17.9	11.3	895.8	3.7	16.2	11.1	879.9	3.7	16.2
400	14.1	1117.7	4.6	20.1	12.8	1014.7	4.2	18.4	12.7	1006.8	4.2	18.4
500	15.5	1228.7	5.1	22.3	14.2	1125.7	4.7	20.6	14.1	1117.7	4.7	20.6
600	16.6	1315.9	5.5	24.1	15.5	1228.7	5.1	22.3	15.5	1228.7	5.1	22.3
700	17.7	1403.1	5.8	25.4	16.4	1300.1	5.5	24.1	16.4	1300.1	5.5	24.1

Table 4: Raw data and calculated values of V_{rf} and I_{rf}, for the experiment conducted with plasma present at 10, 30, and 50 mTorr.

Figures 7 and 8 are plots of V_{rf} and I_{rf} as functions of P, the power dissipated in the coil. The plots are linear, as anticipated, showing increasing voltage and current with increased power.

The total inductance seen in the primary circuit, L_s, is calculated by equation (11), substituting for V_{rf}, I_{rf}, and P, those values recorded in Table 4. Table 5 contains the calculated values of L_s for plasma pressures of 10, 30, and 50 mTorr, as a function of the power transmitted to the coil.

P [W]	Ls [nH] 10 mTorr	Ls [nH] 30 mTorr	Ls [nH] 50 mTorr
20	671.5	648.5	649.1
50	630.6	637.9	647.5
80	630.6	664.4	628.6
100	645.0	629.7	637.8
200	643.8	624.5	630.9
300	648.2	649.3	637.8
400	651.7	647.9	642.8
500	646.1	642.3	637.8
600	641.7	656.1	646.1
700	648.8	633.9	633.9

Table 5: Total inductance as seen in the primary circuit as a function of power and pressure.

The calculated uncertainty in L_s varies from 0.7% to 1.3%. χ is the change in the primary reactance due to plasma loading and is calculated as

$$\chi = \omega L_S - \omega L_0 \tag{13}$$

Where χ is calculated, the average value of L_0 is used.

The power absorbed by the plasma differs from the power incident on the driving coil, and can be calculated by subtracting the measured power when no plasma is present from that measured when plasma is present in the chamber, for equal values of I_{rf}. Finding the absorbed power allows for the determination of the change in resistance due to plasma loading, ρ, as follows.

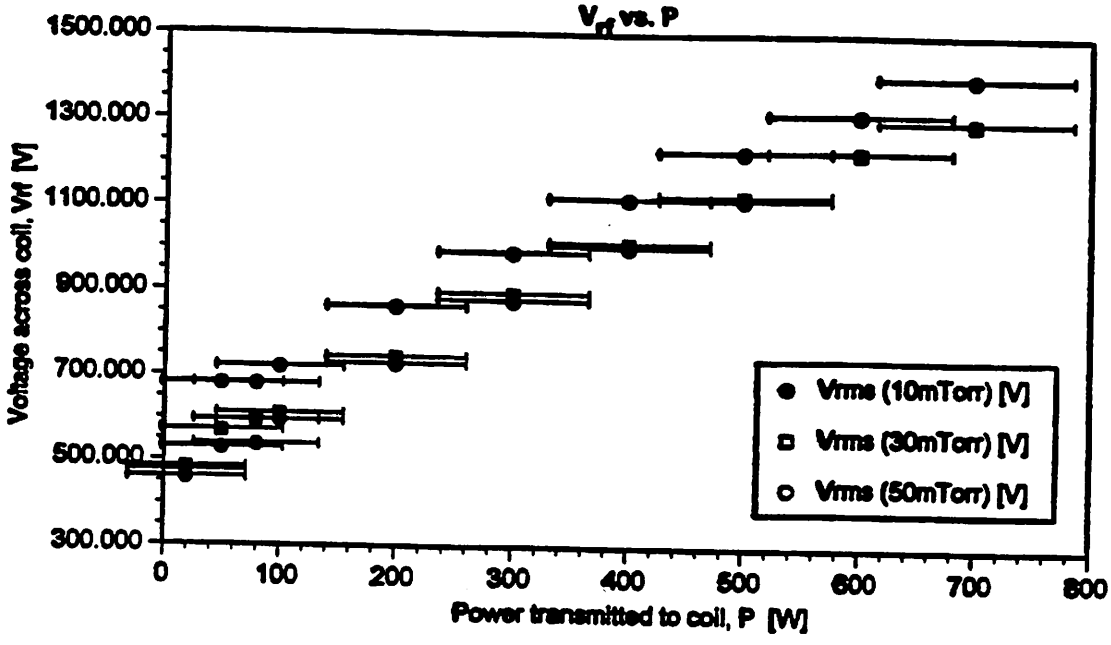

Fig. 7: Voltage as a function of the power transmitted to the coil, with plasma present.

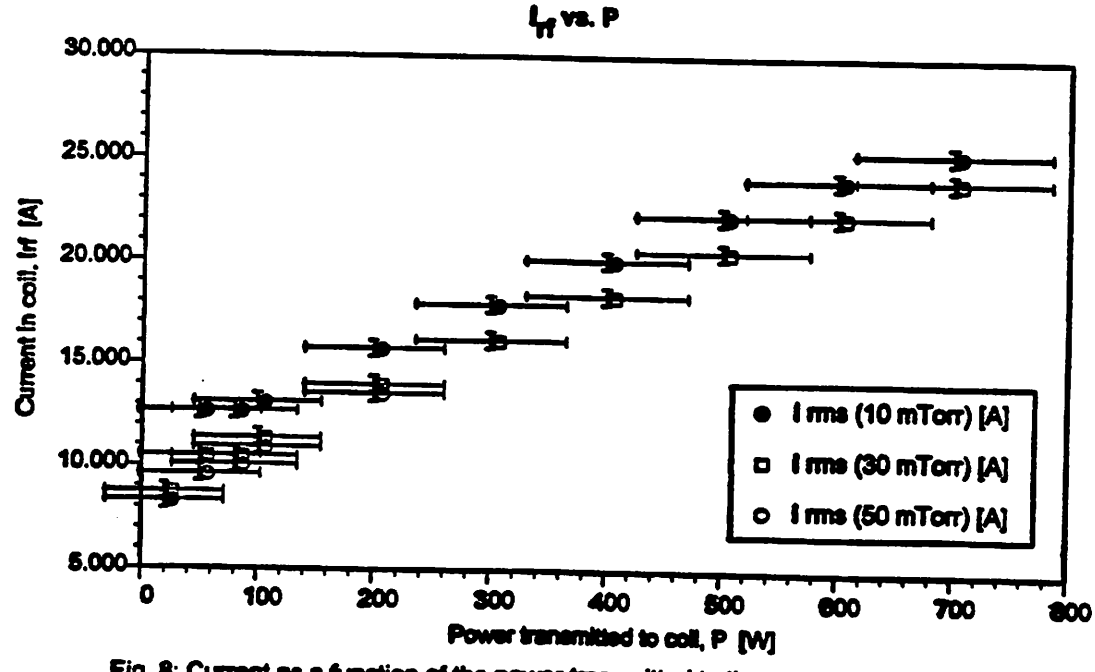

Fig. 8: Current as a function of the power transmitted to the coil, with plasma present.

$$P_{abs} = P_{with\ plasma} - P_{without\ plasma} = R_1 I_{rf}^2 - R_0 I_{rf}^2 \tag{14}$$

R_1 is the total resistance seen in the primary circuit when plasma is present and inductive coupling is taking place. R_1-$R_0 = \rho$, therefore,

$$\rho = \frac{P_{abs}}{|I_{rf}|^2} \tag{15}$$

The values of P_{abs}, $-\chi$, and ρ as functions of the power transmitted to the coil, and plasma pressure are summarized in Table 6.

	10 mTorr			30 mTorr			50 mTorr		
P[W]	P_{abs}[W]	-χ[Ω]	ρ[Ω]	P_{abs}[W]	-χ[Ω]	ρ[Ω]	P_{abs}[W]	-χ[Ω]	ρ[Ω]
20	39.8	-1.23	0.58	33.9	0.72	0.44	39.8	0.67	0.58
50	10.2	2.25	0.06	40.0	1.63	0.36	51.9	0.81	0.56
80	40.2	2.25	0.25	70.0	-0.63	0.64	76.0	2.42	0.75
100	54.3	1.03	0.32	78.1	2.33	0.60	84.1	1.63	0.70
200	118.5	1.13	0.48	142.4	2.77	0.73	148.3	2.22	0.81
300	188.8	0.75	0.59	212.6	0.66	0.81	212.6	1.64	0.81
400	259.0	0.45	0.64	282.8	0.78	0.84	282.8	1.21	0.84
500	329.2	0.93	0.66	353.0	1.25	0.84	353.0	1.64	0.83
600	405.4	1.31	0.70	429.2	0.93	0.86	429.2	0.93	0.86
700	487.5	0.70	0.76	505.4	1.97	0.87	505.4	1.97	0.87

Table 6: Absorbed power, $-\chi$, and ρ as a function of power and pressure.

Figures 9, 10, and 11 are plots of ρ as a function of absorbed power for the three gas pressures. The uncertainty in the absorbed power is due to the large uncertainties in the transmitted power measurements, and varies from 20% for larger values of P_{abs}, to 190% for smaller values. Because the calculation of ρ involves the absorbed power values, the uncertainty in ρ is also large, varying between 20% and 137%. Despite the large uncertainties, a trend in the data is observed, where the change in the primary resistance increases with increased absorbed power.

Figures 12, 13, and 14 are plots of $-\chi$ vs. absorbed power. The change in the reactance, χ, is very small, and so even the moderate uncertainties in L_0 and L_s of 0.5% and 1.3%, are large enough, so that when propagated through, the result is a large percentage error in χ that varies from 26% to 133%. Unfortunately, it is not clear whether there exists a correlation between the change in

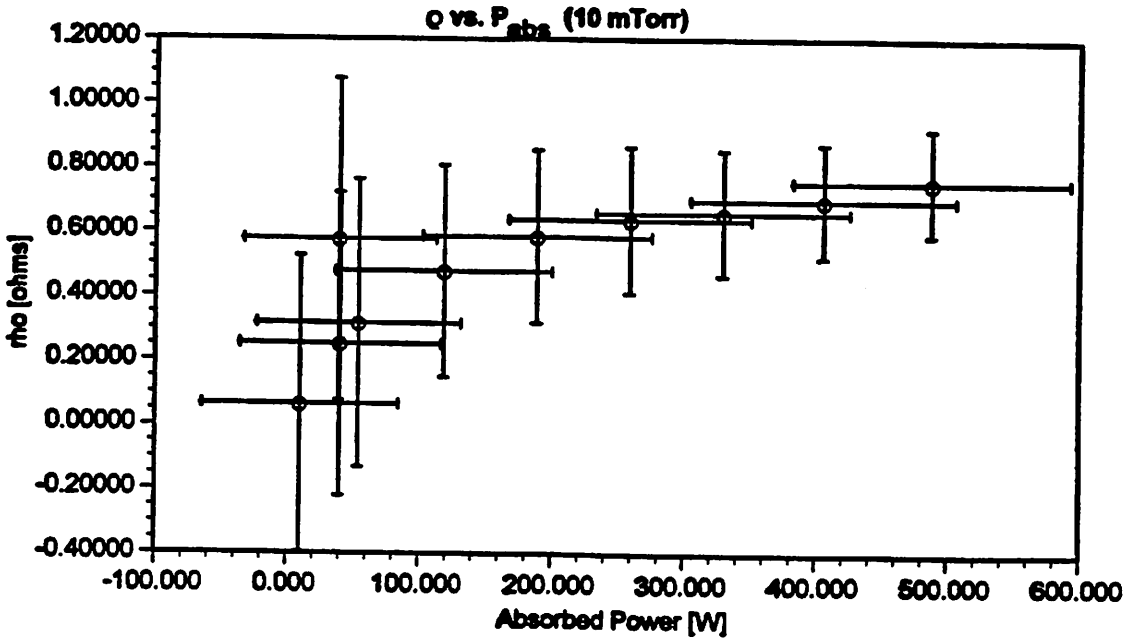

Fig. 9: The change in the primary resistance vs. absorbed power for a pressure of 10 mTorr.

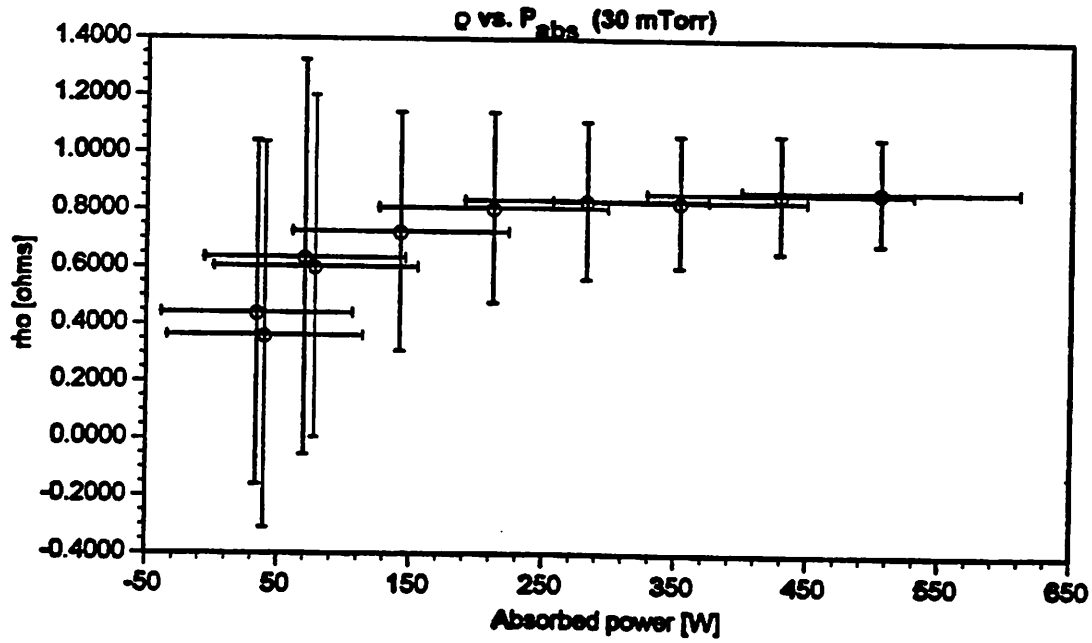

Fig. 10: The change in primary resistance vs. absorbed power for a pressure of 30 mTorr.

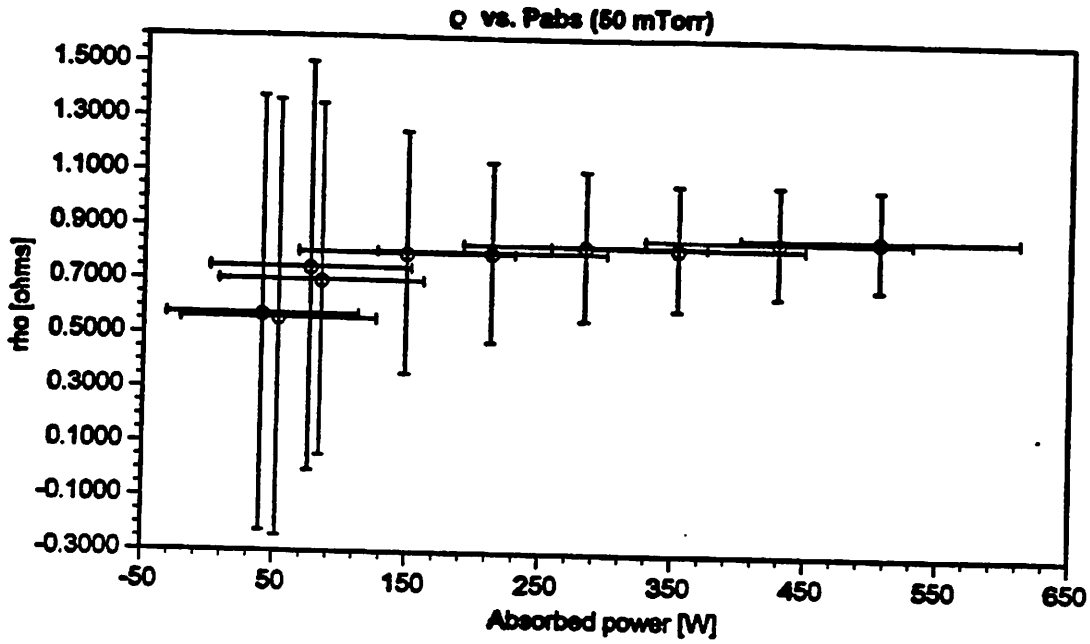

Fig. 11: The change in primary resistance vs. absorbed power at 50 mTorr.

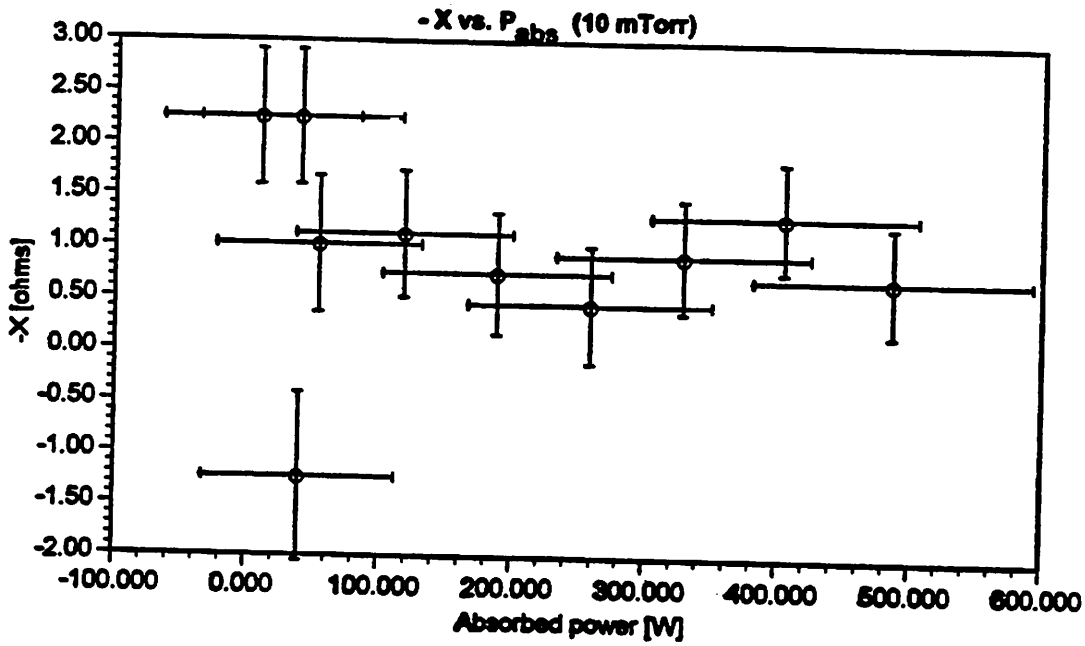

Fig. 12: The change in primary reactance vs. absorbed power at 10 mTorr.

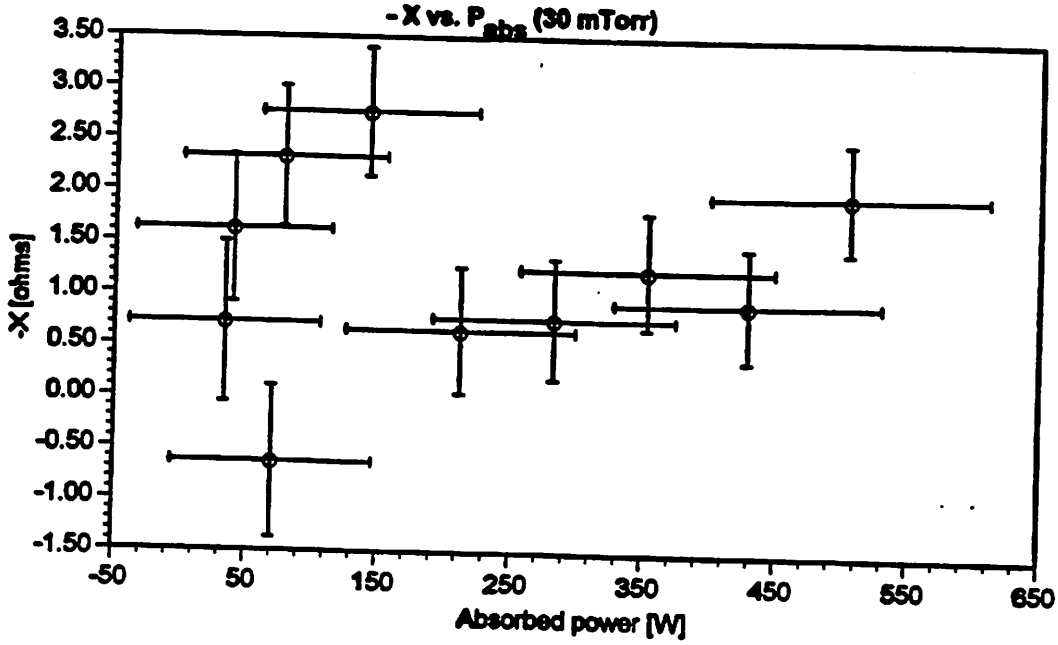

Fig. 13: The change in primary reactance vs. absorbed power at 30 mTorr.

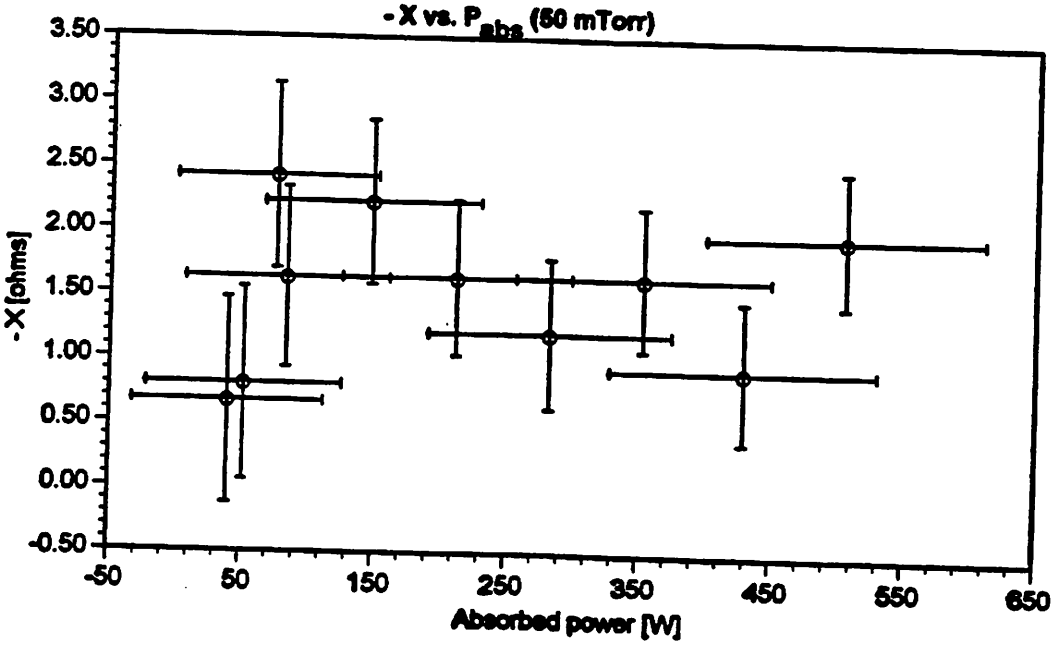

Fig. 14: The change in primary reactance vs. absorbed power at 50 mTorr.

primary reactance and the absorbed power. A more precise measurement of the transmitted power and a larger collection of data may yield better results.

IV. Conclusion

Inductive discharges have been studied using a Transformer Coupled Plasma source powered at 13.56 MHz, where the inductive coupling process between the driving coil and the plasma is modeled as an air-core transformer. The effect of the plasma loading is seen in the primary circuit as a change in the impedance by an amount of $\rho + j\chi$. The purpose of the investigation is to observe this effect, and the correlations between ρ and χ, and the absorbed power. This is achieved by relating the external electrical quantities of voltage, current, and transmitted power, and the calculated characteristics of the driving coil. In order to accomplish this task, a shielded voltage divider was designed and constructed to produce a reliable measurement of the voltage across the driving coil despite the large amount of rf interference produced by the high-power rf inductive coupling. The voltage division was determined for a driving frequency of 13.56 MHz to be -47.01 dB ± 0.02 dB. The experiment was conducted where the coil current, the voltage, and the transmitted power were recorded when no plasma was present in the reaction chamber. This data yielded the values of R_0, the coil resistance, and L_0, the coil inductance. The experiment was repeated with plasma present within the chamber at pressures of 10, 30, and 50 mTorr. A comparison with the data collected with no plasma present, allowed for the determination of the effect of plasma loading. The change in primary impedance was calculated and plotted as a function of absorbed power. A correlation between ρ and the absorbed power was observed, with increasing change in primary resistance for increased absorbed power. A correlation between the change in the primary reactance and the absorbed power was not observed. This may be due to the large error present in the transmitted power measurements.